



# Reversible lysine fatty acylation of an anchoring protein mediates adipocyte adrenergic signaling

Rushita A. Bagchi<sup>a,b,1</sup>, Emma L. Robinson<sup>a,b</sup>, Tianjing Hu<sup>a,b</sup>, Ji Cao<sup>c,2</sup>, Jun Young Hong<sup>c</sup>, Charles A. Tharp<sup>a,b</sup>, Hanan Qasim<sup>d</sup>, Kathleen M. Gavin<sup>e,f</sup>, Julie Pires da Silva<sup>a</sup>, Jennifer L. Major<sup>a,b</sup>, Bradley K. McConnell<sup>d</sup>, Edward Seto<sup>g</sup>, Hening Lin<sup>c,h</sup>, and Timothy A. McKinsey<sup>a,b,3</sup>

<sup>a</sup>Department of Medicine, Division of Cardiology, University of Colorado Anschutz Medical Campus, Aurora, CO 80045-2507; <sup>b</sup>Consortium for Fibrosis Research & Translation, University of Colorado Anschutz Medical Campus, Aurora, CO 80045-2507; <sup>c</sup>Department of Chemistry and Chemical Biology, Cornell University, Ithaca, NY 14853; <sup>d</sup>Department of Pharmacological and Pharmaceutical Sciences, University of Houston College of Pharmacy, Houston, TX 77204-5037; <sup>e</sup>Department of Medicine, Division of Geriatric Medicine, University of Colorado Anschutz Medical Campus, Aurora, CO 80045-2507; <sup>f</sup>Eastern Colorado Geriatric Research, Education and Clinical Center, Rocky Mountain Regional Veterans Affairs Medical Center, Aurora, CO 80045; <sup>g</sup>Department of Biochemistry and Molecular Medicine, The George Washington University School of Medicine and Health Sciences, Washington, DC 20037; and <sup>h</sup>HHMI, Cornell University, Ithaca, NY 14853

Edited by Brian Kobilka, Department of Molecular and Cellular Physiology, Stanford University School of Medicine, Stanford, CA; received November 1, 2021; accepted December 8, 2021

***N*-myristoylation on glycine is an irreversible modification that has long been recognized to govern protein localization and function. In contrast, the biological roles of lysine myristoylation remain ill-defined. We demonstrate that the cytoplasmic scaffolding protein, gravin- $\alpha$ /A kinase-anchoring protein 12, is myristoylated on two lysine residues embedded in its carboxyl-terminal protein kinase A (PKA) binding domain. Histone deacetylase 11 (HDAC11) docks to an adjacent region of gravin- $\alpha$  and demyristoylates these sites. In brown and white adipocytes, lysine myristoylation of gravin- $\alpha$  is required for signaling via  $\beta_2$ - and  $\beta_3$ -adrenergic receptors ( $\beta$ -ARs), which are G protein-coupled receptors (GPCRs). Lysine myristoylation of gravin- $\alpha$  drives  $\beta$ -ARs to lipid raft membrane microdomains, which results in PKA activation and downstream signaling that culminates in protective thermogenic gene expression. These findings define reversible lysine myristoylation as a mechanism for controlling GPCR signaling and highlight the potential of inhibiting HDAC11 to manipulate adipocyte phenotypes for therapeutic purposes.**

lysine myristoylation | signal transduction | adrenergic receptor | HDAC11

**N**-myristoylation is the covalent linkage of the 14-carbon fatty acid, myristate, via an amide bond to glycine at position 2 of proteins harboring the consensus motif, Met-Gly-X-X-Ser/Thr. This fatty acylation process is catalyzed by *N*-myristoyltransferases 1 and 2 (NMT1 and NMT2) and occurs cotranslationally following removal of the initiator methionine by methionine aminopeptidase (1). *N*-myristoylation has diverse consequences (2), such as altering protein stability and protein-protein interactions, but is best known for its impact on protein subcellular distribution and membrane localization, as exemplified by the role of glycine-2 myristoylation in targeting members of the Src family of protein tyrosine kinases to the inner surface of the plasma membrane to initiate signal transduction (3). NMT-mediated *N*-myristoylation was also recently described to occur on lysine-3 of adenosine diphosphate-ribosylation factor 6 (ARF6) (4, 5), thereby expanding the repertoire of targets and regulatory processes that are controlled by this posttranslational modification (PTM).

It has been recognized for nearly 30 y that internal lysine residues in proteins can also be myristoylated (6, 7), but there remains a paucity of information on the function and regulation of this fatty acylation event when it occurs distal to *N* termini. Lysine fatty acylation of tumor necrosis factor- $\alpha$  (TNF- $\alpha$ ) blocks its secretion from cells and targets the cytokine for lysosomal degradation (8, 9), while fatty acylation of the ras-related protein, R-Ras2, on lysines near its carboxyl terminus drives the protein to the plasma membrane, where it stimulates the phosphatidylinositol 3-kinase (PI3K)/AKT signaling pathway (10).

The extent to which internal lysine fatty acylation regulates proteins beyond these examples is unclear.

Although the identity of myristoyltransferases that govern internal lysine myristoylation is unknown, knowledge about the demyristoylases is emerging, with certain members of the histone deacetylase (HDAC) superfamily exhibiting potent lysine defatty-acylase activity (11). Eighteen mammalian HDACs are encoded by distinct genes and are grouped into four classes. Class I, II, and IV HDACs are zinc-dependent enzymes, while class III HDACs, which are also known as sirtuins (SIRT),

## Significance

Recently, histone deacetylase 11 (HDAC11) was shown to function as an enzyme that removes lipids such as myristoyl groups from lysines in proteins, yet only one substrate of HDAC11 has been reported. Here, we define gravin- $\alpha$ /A kinase-anchoring protein 12 as a second HDAC11 substrate. By demyristoylating gravin- $\alpha$  in adipocytes, HDAC11 prevents  $\beta$ -adrenergic receptors ( $\beta$ -ARs), which are G protein-coupled receptors (GPCRs), from translocating to membrane microdomains that are required for downstream protective signaling by protein kinase A (PKA). These findings demonstrate a role for reversible lysine myristoylation in the control of GPCR signaling and lay the foundation for developing therapeutics for obesity based on enhancing  $\beta$ -AR signaling in adipose tissue by manipulating the HDAC11:gravin- $\alpha$  axis.

Author contributions: R.A.B., E.L.R., B.K.M., H.L., and T.A.M. designed research; R.A.B., E.L.R., T.H., J.C., J.Y.H., C.A.T., H.Q., J.P.d.S., and J.L.M. performed research; K.M.G., B.K.M., E.S., and H.L. contributed new reagents/analytic tools; R.A.B., E.L.R., T.H., J.C., J.Y.H., C.A.T., H.Q., J.L.M., B.K.M., H.L., and T.A.M. analyzed data; and R.A.B., E.L.R., J.Y.H., C.A.T., H.Q., H.L., and T.A.M. wrote the paper.

Competing interest statement: T.A.M. is on the scientific advisory boards of Artemes Bio, Inc., and Eikonizo Therapeutics, received funding from Italfarmaco for an unrelated project, and has a subcontract from Eikonizo Therapeutics related to a Small Business Innovation Research grant from the NIH (HL154959). H.L. is a founder and consultant for Sedec Therapeutics.

This article is a PNAS Direct Submission.

This article is distributed under Creative Commons Attribution-NonCommercial-NoDerivatives License 4.0 (CC BY-NC-ND).

<sup>1</sup>Present address: Department of Internal Medicine, College of Medicine, University of Arkansas for Medical Sciences, Little Rock, AR 72205.

<sup>2</sup>Present address: Zhejiang Province Key Laboratory of Anti-Cancer Drug Research, College of Pharmaceutical Sciences, Zhejiang University, Hangzhou 310058, China.

<sup>3</sup>To whom correspondence may be addressed. Email: timothy.mckinsey@cuanschutz.edu.

This article contains supporting information online at <http://www.pnas.org/lookup/suppl/doi:10.1073/pnas.2119678119/-DCSupplemental>.

Published February 11, 2022.

require nicotinamide adenine dinucleotide (NAD<sup>+</sup>) for catalytic activity (12). Many HDACs display substrate specificity toward acyl groups other than acetyl. For example, SIRT5 functions as a lysine desuccinylase and demalonylase (13), while SIRT6 is a lysine demyristoylase with the ability to target myristoyl-lysines in TNF- $\alpha$  and R-Ras2 (8, 10). Among the zinc-dependent HDACs, HDAC8 possesses demyristoylase activity *in vitro*, and three recent reports established that HDAC11 is a robust lysine demyristoylase (14–16) with a catalytic efficiency >10,000-fold higher for myristoyl-lysine versus acetyl-lysine. The only known substrate of HDAC11 is serine hydroxymethyltransferase-2 (SHMT2), which regulates interferon signaling (14).

The discovery of HDAC11 as a lysine demyristoylase provides an opportunity to uncover biological roles of lysine myristoylation, which heretofore remains an elusive PTM, and to address the potential of inhibiting lysine demyristoylase activity for therapeutic purposes. In this regard, we recently found that global deletion of HDAC11 in mice prevented weight gain and improved overall metabolic health in the face of chronic high-fat feeding (17, 18). The salutary effects of HDAC11 knockout (KO) were linked to increased abundance and function of brown adipose tissue (BAT). In contrast to white adipose tissue (WAT), which functions mainly to store energy in the form of triglycerides, BAT is highly metabolically active and produces heat through nonshivering thermogenesis via uncoupling protein-1 (UCP1). HDAC11 suppressed UCP1 gene expression through association with the bromodomain and extraterminal (BET) family member, BRD2, in adipocyte nuclei (17).

There is intense interest in developing therapies for obesity based on stimulating BAT function or phenotypic transformation of WAT into “beige” fat to promote energy expenditure (19), and preclinical studies have established stimulation of  $\beta$ -adrenergic receptors ( $\beta$ -ARs) as a robust approach to achieve this goal (20). However, agonists of these G protein-coupled receptors (GPCRs) have underperformed in clinical studies of obese individuals (21), emphasizing the need to better understand the molecular underpinnings of thermogenic signaling in adipocytes. Here, we describe a cytoplasmic function for HDAC11 in the control of adipocyte  $\beta$ -AR signaling. By demyristoylating two lysine residues within the protein kinase A (PKA) binding domain of the scaffolding protein, gravin- $\alpha$ /AKAP12, HDAC11 prevents gravin- $\alpha$ : $\beta$ -AR:PKA complexes from localizing to membrane lipid rafts that are required to stimulate downstream signaling. Conversely, selective pharmacological inhibition of HDAC11 drives the complexes to lipid rafts to promote  $\beta$ -AR signaling and thermogenic gene expression. These findings establish myristoylation of internal lysine residues in gravin- $\alpha$  as a reversible and druggable mechanism for controlling GPCR signaling.

## Results

**Nuclear and Cytoplasmic HDAC11 Are Capable of Blocking  $\beta_3$ -AR-Mediated UCP1 Induction.** Our prior work with ectopically expressed HDAC11 demonstrated that a nuclear pool of the protein associates with BRD2 to repress expression of UCP1 in adipocytes (17). Consistent with this, indirect immunofluorescence (IF) imaging of primary adipocytes derived from wild-type (WT) mouse interscapular BAT (iBAT), inguinal WAT (ingWAT), and epididymal WAT (eWAT) revealed prominent nuclear localization of endogenous HDAC11 (Fig. 1*A*, *Upper*). However, significant HDAC11 staining was also observed in the cytoplasmic compartments of each adipocyte type, suggesting extranuclear functions for the enzyme. Parallel imaging of cells obtained from *Hdac11* KO mice confirmed the specificity of staining (Fig. 1*A*, *Lower*).

To address the relative contributions of nuclear and cytoplasmic HDAC11 in the control of signal-induced thermogenic gene expression, lentiviruses were constructed to express WT HDAC11 or versions of HDAC11 fused to a heterologous nuclear export sequence (NES) or a nuclear localization signal (NLS) (Fig. 1*B*). IF and cellular fractionation studies with cultured 3T3-L1 white adipocytes confirmed that lentiviral HDAC11 WT was present in both the nucleus and cytoplasm, while HDAC11 NES and NLS were exclusively cytoplasmic or nuclear, respectively (Fig. 1*C* and *D*). Next, 3T3-L1 cells or HIB1B brown adipocytes were infected with the lentiviruses or viruses encoding catalytically inactive (H143A) versions of HDAC11 WT, NES, or NLS, and the cells were subsequently stimulated with the  $\beta_3$ -AR agonist CL-316,243 (CL) (Fig. 1*E*). Remarkably, each HDAC11 construct blocked CL-induced UCP1 protein expression in both cell types in a manner that was dependent on HDAC11 catalytic activity (Fig. 1*F* and *G*); basal UCP1 protein expression was higher in HIB1B cells, which is consistent with their BAT-like characteristics (22). These data suggest that, in addition to directly repressing UCP1 gene expression in the nucleus, HDAC11 functions in the cytoplasm to suppress  $\beta$ -AR-mediated thermogenic gene expression in adipocytes.

## Gravin- $\alpha$ /AKAP12 Myristoylation Is Induced upon HDAC11 Inhibition.

HDAC11 is a weak deacetylase but is a potent lysine defattyacylase (14–16). To search for putative cytoplasmic substrates of HDAC11, sequential click chemistry with an Alk-14 tag followed by mass spectrometry of metabolically labeled proteins was performed with mouse embryonic fibroblasts, focusing on proteins with increased fatty acylation upon knockdown of HDAC11 expression (*SI Appendix*, Fig. S1*A*). Among the proteins that were enriched upon HDAC11 knockdown was gravin- $\alpha$ /AKAP12 (*SI Appendix*, Fig. S1*B* and *Dataset S1*), which has previously been shown to regulate  $\beta_2$ -AR desensitization, sequestration, resensitization, and cAMP recovery rate following agonist stimulation (23–26). Coimmunoprecipitation (co-IP) studies with lentiviral-infected 3T3-L1 cells demonstrated that endogenous gravin- $\alpha$  associates with HDAC11 WT and NES but not HDAC11 NLS (*SI Appendix*, *Supplementary Index* and Fig. S1*B* and *C*). In contrast, HDAC11 WT and NLS, but not NES, associated with BRD2. These findings suggested the possibility that cytoplasmic HDAC11 regulates adipocyte  $\beta$ -AR signaling via gravin- $\alpha$ .

To specifically address the potential of HDAC11 to regulate gravin- $\alpha$  myristoylation in adipocytes, studies were performed with a “clickable” Alk-12 and 3T3-L1 or HIB1B cells treated with FT895, a highly selective small-molecule inhibitor of HDAC11 (Fig. 2*A*) (27). Three hours of FT895 treatment led to robust myristoylation of gravin- $\alpha$  in 3T3-L1 cells, and the signal persisted until 12 h posttreatment (Fig. 2*B*). We note that in this experiment, and in others throughout the manuscript, multiple forms of gravin- $\alpha$  were detected by immunoblotting. Full-length gravin- $\alpha$  migrates at ~250 kDa in sodium dodecyl sulfate-polyacrylamide gel electrophoresis gels, but gravin- $\alpha$  multimers are often revealed in the absence of urea (25). Thus, full-length and multimeric gravin- $\alpha$  are indicated with arrows where necessary.

In HIB1B brown adipocytes, gravin- $\alpha$  was basally myristoylated and inducibly myristoylated following FT895 treatment (Fig. 2*C* and *SI Appendix*, Fig. S2*A*). FT895 also stimulated gravin- $\alpha$  myristoylation in cultured mouse BAT and WAT explants (*SI Appendix*, Fig. S2*B–E*). To address the translational potential of our findings, human visceral adipose tissue (VAT) explants or purified human adipocytes were treated with FT895 in culture (Fig. 2*D* and *E*), and in both sets of samples, HDAC11 inhibition led to an increase in gravin- $\alpha$  myristoylation (Fig. 2*F–H*). To confirm the specificity of the observed effects, primary cultured adipocytes from WT and *Hdac11* KO

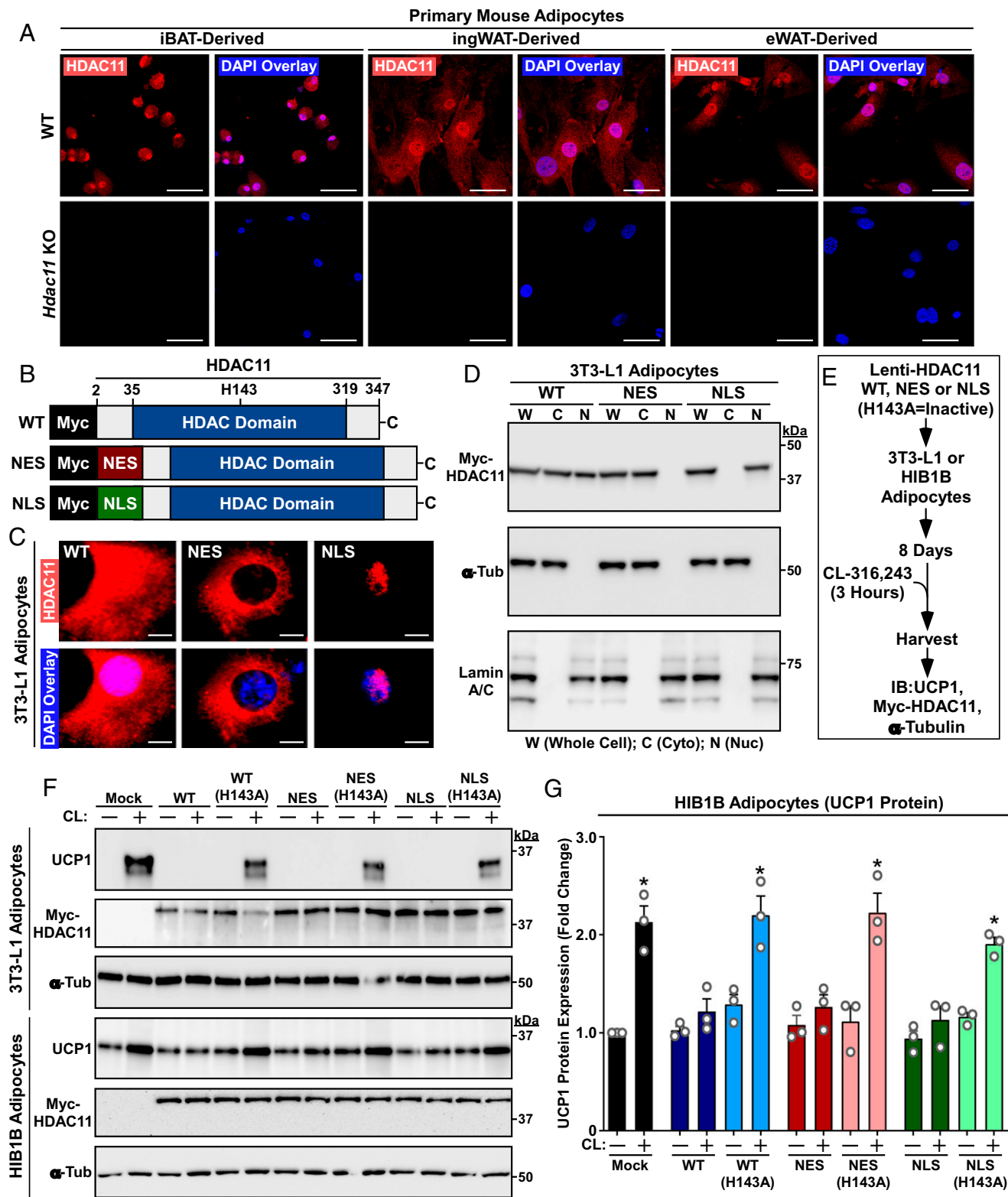


**Fig. 1.** Nuclear and cytoplasmic HDAC11 are capable of blocking  $\beta_3$ -AR-mediated UCP1 induction. (A) Indirect immunofluorescence of endogenous HDAC11 in primary mouse adipocytes derived from adipose depots of WT or *Hdac11* KO mice. Nuclei were stained with DAPI. (Scale bar, 50  $\mu$ m.) (B) Schematic representation of Myc-tagged human HDAC11 expression constructs. Conversion of histidine-143 to alanine (H143A) renders HDAC11 catalytically inactive. (C) Indirect immunofluorescence of Myc-tagged HDAC11 in 3T3-L1 adipocytes. (Scale bar, 10  $\mu$ m.) (D) Immunoblots confirming expression of Myc-tagged HDAC11 in the predicted subcellular fractions of 3T3-L1 adipocytes.  $\alpha$ -Tubulin and lamin A/C served as controls for the purity of cytoplasmic and nuclear fractions, respectively. (E) Schematic depiction of the  $\beta_3$ -AR signaling experiment. (F) Immunoblot analysis of 3T3-L1 white adipocyte and HIB1B brown adipocyte homogenates. (G) Quantification of UCP1 protein in three independent experiments with HIB1B cells. Each N = an independent plate of cells. Data are presented as mean + SEM; \* $P \leq 0.05$  versus unstimulated controls in each condition. Please visit Figshare for a higher-resolution version (10.6084/m9.figshare.19082813).

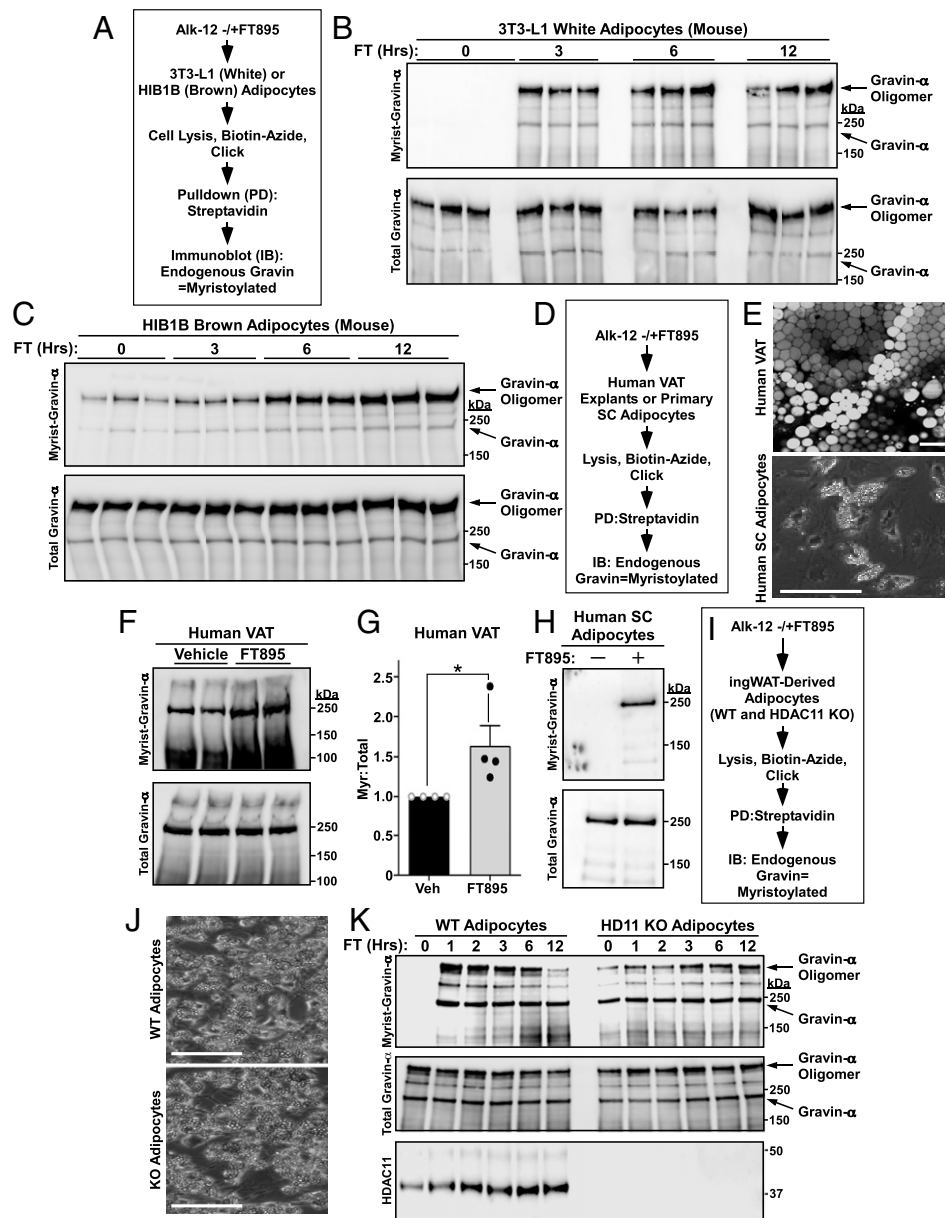


**Fig. 2.** Gravin- $\alpha$ /AKAP12 myristoylation is induced upon HDAC11 inhibition. (A) Schematic depiction of the click chemistry experiment employed to assess gravin- $\alpha$  myristoylation in 3T3-L1 and HIB1B adipocytes. Cells were treated with 10  $\mu$ M FT895 for the indicated times. (B) Immunoblot analysis of 3T3-L1 adipocyte homogenates. FT, FT895; Hrs, hours; Myrist, myristoylated. (C) Immunoblot analysis of HIB1B adipocyte homogenates. (D) Schematic depiction of the click chemistry experiment to assess gravin- $\alpha$  myristoylation in human adipose tissue explants and purified adipocytes. Explants and cells were treated with 100  $\mu$ M and 10  $\mu$ M FT895 for 12 h, respectively. SC, subcutaneous. (E, Top) Representative whole mount human visceral adipose tissue (VAT) confocal microscopy image with BODIPY 493/503 (lipid droplet) staining; 20 $\times$  objective lens. (Scale bar, 100  $\mu$ m.) (Lower) Representative brightfield microscopy image of differentiated human SC stromal vascular fraction (SVF)-derived adipocytes; 10 $\times$  objective lens. (Scale bar, 400  $\mu$ m.) (F) Immunoblot analysis of VAT homogenates. (G) Densitometry quantification of myristoylated gravin- $\alpha$  relative to total gravin- $\alpha$  protein in human VAT explants. Data are represented as means  $\pm$  SEM.  $n = 4$  per condition; \* $P < 0.05$  compared to untreated. Veh, vehicle. (H) Immunoblot analysis of human SC adipocyte homogenates. (I) Schematic depiction of the click chemistry experiment to assess gravin- $\alpha$  myristoylation in cultured adipocytes derived from WT and *Hdac11* KO ingWAT. Cells were treated with 10  $\mu$ M FT895 for the indicated times. (J) Brightfield microscopy images of differentiated adipocytes derived from WT and *Hdac11* KO ingWAT. (Scale bar, 400  $\mu$ m.) (K) Immunoblot analysis of homogenates from adipocytes treated for the indicated times with 10  $\mu$ M FT895. Please visit Figshare for a higher-resolution version (10.6084/m9.figshare.19082813).

mice were treated with FT895 (Fig. 2 I and J). Gravin- $\alpha$  myristoylation was undetectable basally in WT adipocytes but was rapidly and robustly induced following FT895 treatment (Fig. 2K). Conversely, gravin- $\alpha$  was highly basally myristoylated in *Hdac11* KO adipocytes, and FT895 failed to further increase myristoylation of the protein. Notably, the apparent differences in oligomer myristoylation in WT and KO cells at 12 h (Fig. 2 K, Upper) appear to correlate with altered total levels

of oligomer (Fig. 2 K, Middle) and thus do not reflect true changes in gravin- $\alpha$  myristoylation. Collectively, these findings strongly suggest that HDAC11 suppresses gravin- $\alpha$  myristoylation.

**HDAC11 Demyristoylates Two Lysines in the PKA Binding Domain of Gravin- $\alpha$ .** Gravin- $\alpha$  can be *N*-myristoylated on glycine-2 (28), which appears to target the protein to the endoplasmic reticulum,

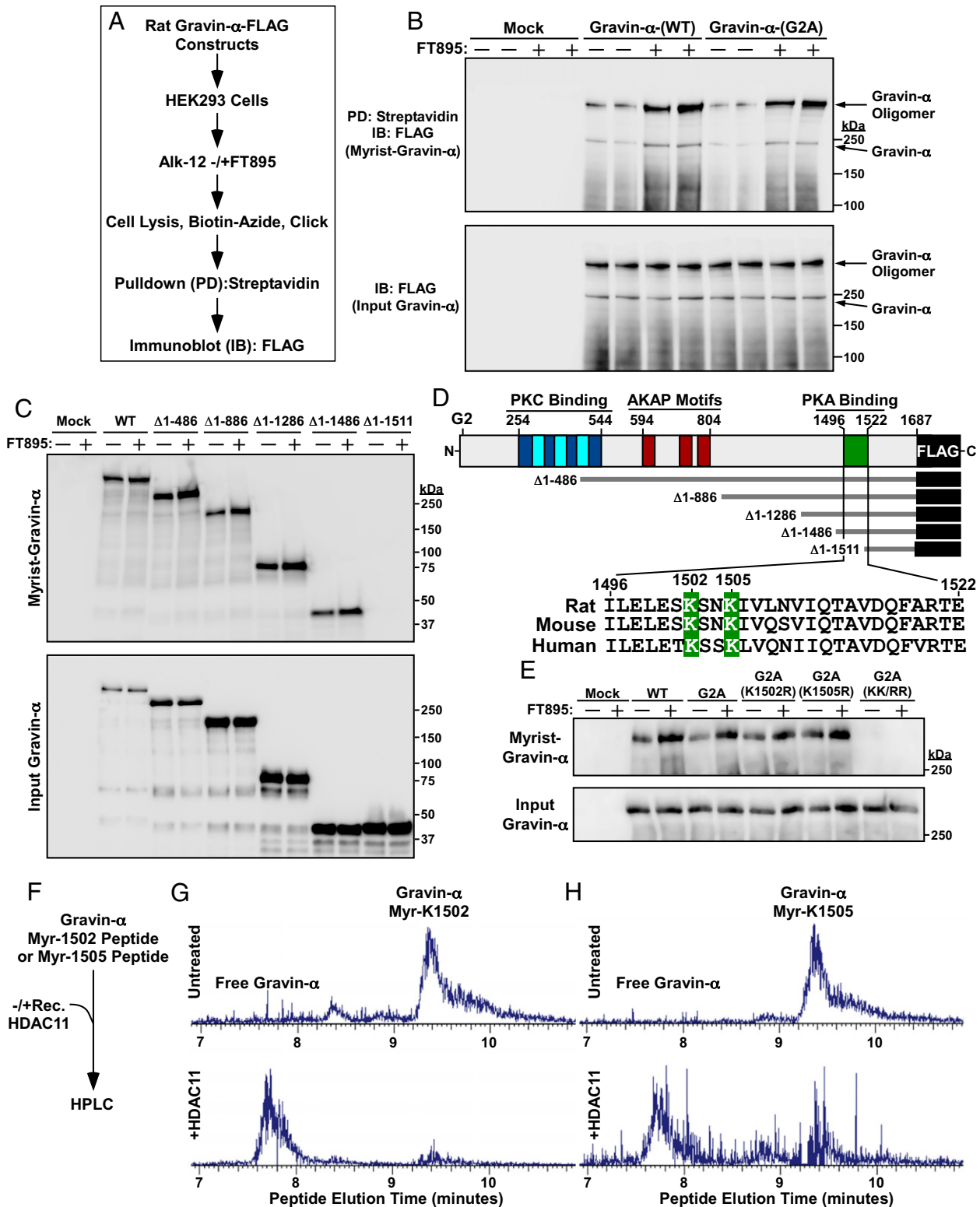


**Fig. 3.** HDAC11 demyristoylates two lysines in the PKA binding domain of gravin- $\alpha$ . (A) Schematic depiction of the experiment to assess myristoylation of ectopically expressed gravin- $\alpha$  constructs. (B) Immunoblot analysis of homogenates of HEK293 cells transfected with the indicated FLAG-tagged gravin- $\alpha$  constructs and treated with vehicle control (-) or 10  $\mu$ M FT895 for 12 h. Myrist, myristoylated. (C) Immunoblot analysis of homogenates of HEK293 cells transfected with the indicated constructs for N-terminally truncated, FLAG-tagged gravin- $\alpha$  and treated with vehicle control (-) or 10  $\mu$ M FT895 for 12 h. (D) Schematic representation of gravin- $\alpha$ , gravin- $\alpha$  constructs, and the conserved lysine myristoylation sites embedded in the PKA binding domain of gravin- $\alpha$ . (E) Immunoblot analysis of homogenates of HEK293 cells transfected with constructs for gravin- $\alpha$  harboring the indicated amino acid substitutions and treated with vehicle control (-) or 10  $\mu$ M FT895 for 12 h. (F) Schematic depiction of the experiment to address whether HDAC11 is capable of directly demyristoylating lysine-1502 and lysine-1505 of gravin- $\alpha$ . (G) LC-MS traces of myristoyl-lysine-1502 peptide and free peptide of gravin- $\alpha$  before and after treatment with recombinant HDAC11 for 1.5 h at 37°C. (H) LC-MS traces of myristoyl-lysine-1505 peptide and free peptide of gravin- $\alpha$  before and after treatment with recombinant HDAC11 for 1.5 h at 37°C. For G and H, peaks were searched using Xcaliber software. Myr, myristoyl. Peaks were searched using Xcaliber software. Please visit Figshare for a higher-resolution version (10.6084/m9.figshare.19082813).

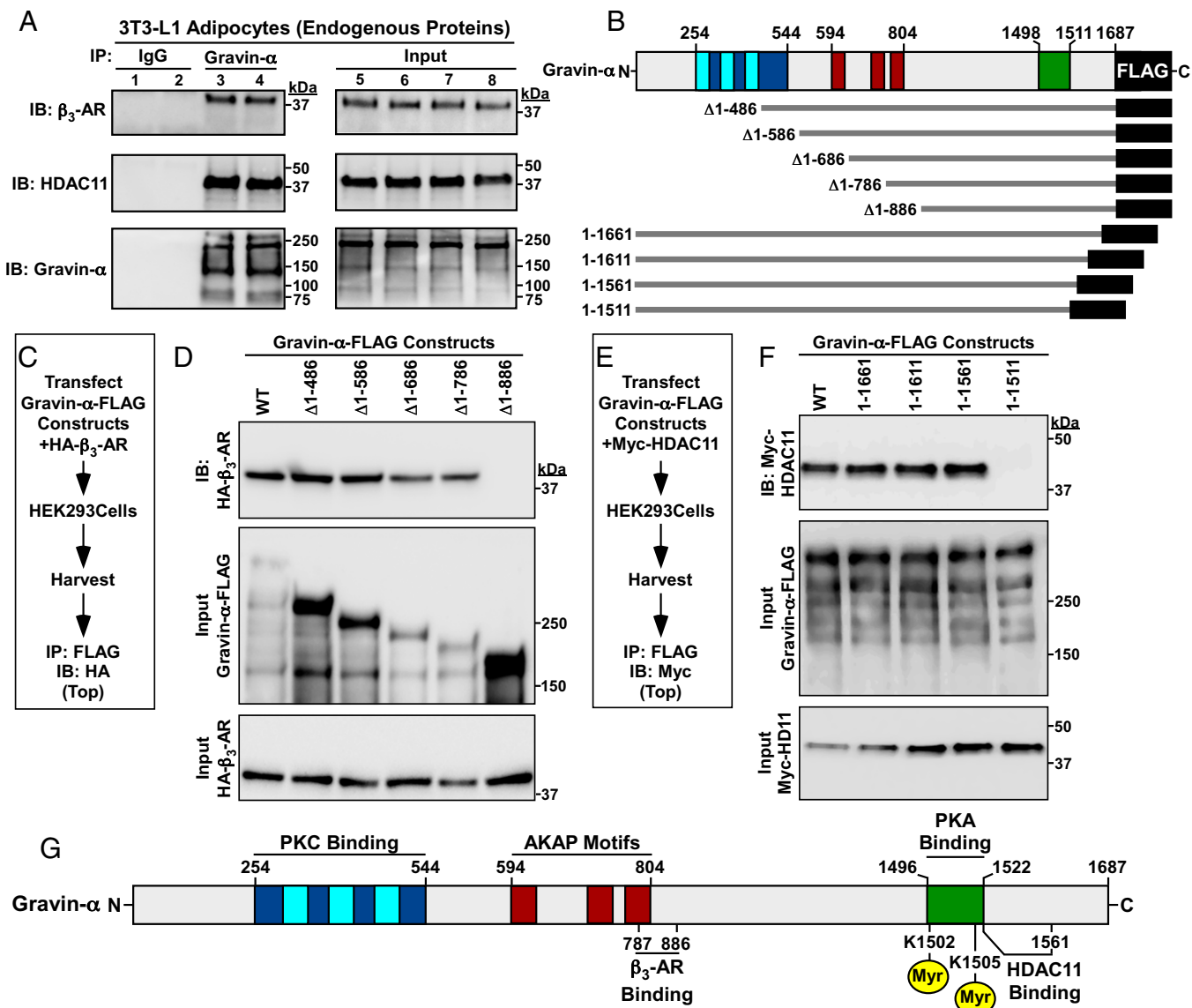


**Fig. 4.** Discrete regions of gravin- $\alpha$  mediate associations with the  $\beta_3$ -AR and HDAC11. (A) Co-IP of endogenous gravin- $\alpha$  with endogenous  $\beta_3$ -AR and HDAC11 in homogenates from 3T3-L1 adipocytes. IP, immunoprecipitation; IB, immunoblotting. (B) Schematic representation of the N- and carboxyl-terminal truncation constructs of FLAG-tagged rat gravin- $\alpha$  that were employed for co-IP studies. (C) Schematic depiction of the experiment to map the  $\beta_3$ -AR binding domain on gravin- $\alpha$ . (D) Immunoblot analysis of ectopically expressed  $\beta_3$ -AR coimmunoprecipitating with the indicated gravin- $\alpha$  constructs in HEK293 cell homogenates. (E) Schematic depiction of the experiment to map the HDAC11 binding domain on gravin- $\alpha$ . (F) Immunoblot analysis of ectopically expressed HDAC11 coimmunoprecipitating with the indicated gravin- $\alpha$  constructs in HEK293 cell homogenates. (G) Schematic representation of gravin- $\alpha$  incorporating the  $\beta_3$ -AR and HDAC11 binding domains. Please visit Figshare for a higher-resolution version (10.6084/m9.figshare.19082813).

intracellular vesicular compartments, and, together with polybasic domains, to the cell periphery (29, 30). However, FT895 equivalently induced myristoylation of WT and a glycine 2-to-alanine substitution (G2A) derivative of gravin- $\alpha$  when the proteins were ectopically expressed in human embryonic kidney 293 (HEK293) cells (Fig. 3A and B), ruling out the possibility that HDAC11 regulates N-myristoylation of the anchoring protein. Evaluation of a series of deletion constructs mapped the myristoylation sites in gravin- $\alpha$  to a region between amino acids 1,487 and 1,511 (Fig. 3C), which resides within a previously defined PKA binding domain (31) and contains two conserved lysine residues at positions 1,502 and 1,505 (Fig. 3D). Lysine-1502-to-Arginine (K1502R) and K1505R versions of gravin- $\alpha$  were still myristoylated in transfected HEK293 cells, but simultaneous conversion of both lysines to arginine (KK/RR) abolished myristoylation of the protein (Fig. 3E). In vitro enzymatic assays employing

recombinant HDAC11 and peptides myristoylated at K1502 or K1505 confirmed that both sites are efficiently demyristoylated by HDAC11 (Fig. 3F-H). These findings demonstrate that gravin- $\alpha$  undergoes HDAC11-reversible myristoylation on two lysines positioned in its PKA binding domain.

**Discrete Regions of Gravin- $\alpha$  Mediate Associations with the  $\beta_3$ -AR and HDAC11.** Endogenous gravin- $\alpha$  co-IPed (coimmunoprecipitated) with endogenous  $\beta_3$ -AR and HDAC11 in cultured 3T3-L1 cells (Fig. 4A), suggesting that the proteins form a signaling complex in adipocytes. Follow-up co-IP studies with ectopically expressed deletion constructs initially mapped the  $\beta_3$ -AR binding domain on gravin- $\alpha$  to amino acids 487 through 886 (SI Appendix, Supplementary Index and Fig. S3A and B), with additional truncations refining the binding site to a 100-amino-acid region (amino acids 787 through 886), which overlap with the AKAP motifs of

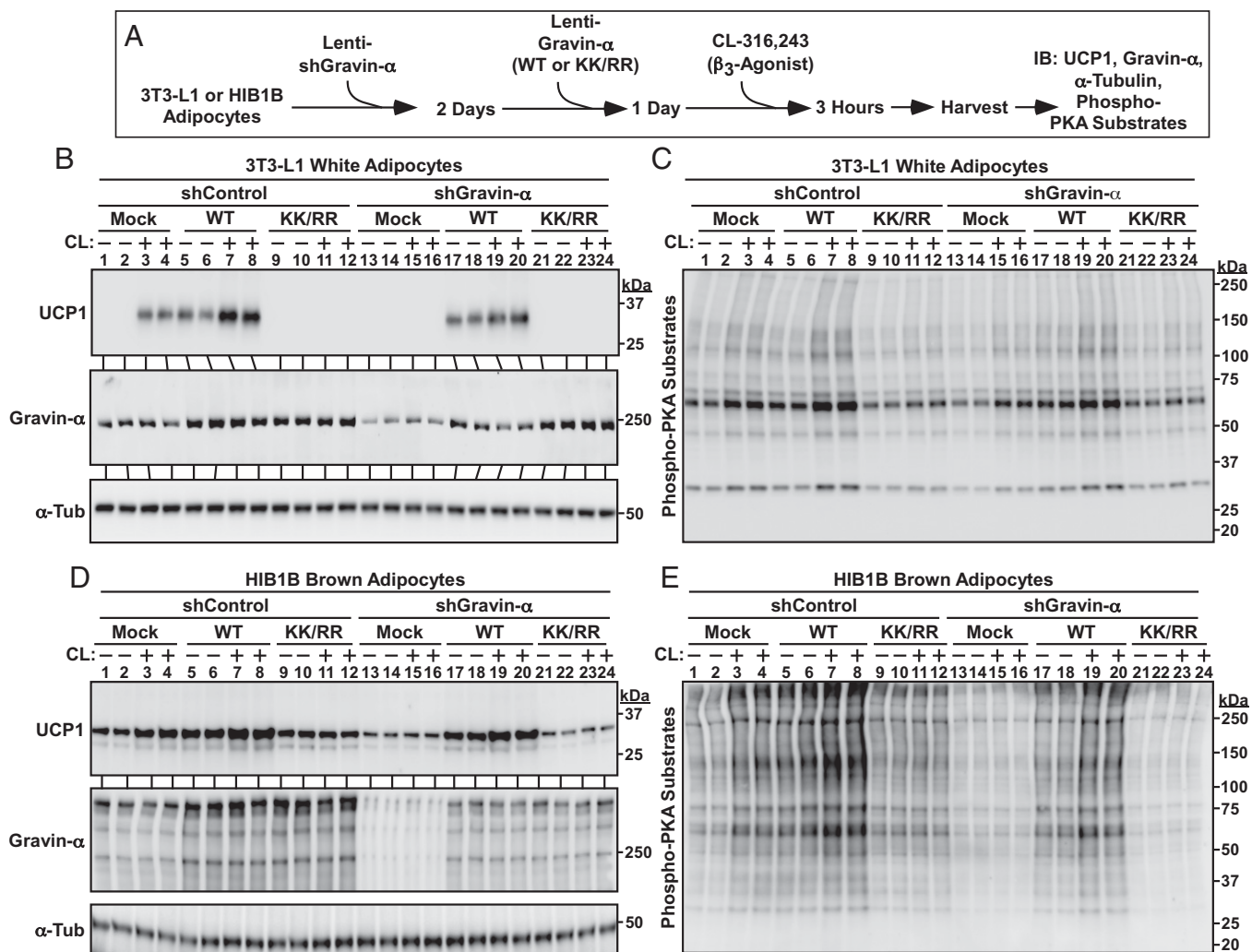


**Fig. 5.** Lysine myristoylation of gravin- $\alpha$  is required for  $\beta_3$ -AR-mediated UCP1 induction. (A) Schematic depiction of the experiment to determine if gravin- $\alpha$  and its myristoylation are required for  $\beta_3$ -AR signaling in adipocytes. (B) Immunoblot analysis of UCP1 induction and gravin- $\alpha$  knockdown in 3T3-L1 adipocytes.  $\alpha$ -Tubulin ( $\alpha$ -Tub) served as a loading control. (C) Immunoblot analysis of 3T3-L1 homogenates using an anti-phospho-PKA substrates antibody. (D) Immunoblot analysis of UCP1 induction and gravin- $\alpha$  knockdown in HIB1B adipocytes.  $\alpha$ -Tub served as a loading control. (E) Immunoblot analysis of HIB1B homogenates using an anti-phospho-PKA substrates antibody. Please visit Figshare for a higher-resolution version (10.6084/m9.figshare.19082813).

the protein (Fig. 4 B–D); AKAP motifs, which are sometimes referred to as WSK motifs, are a core sequence of ~31 amino acids that are conserved in several AKAPs (25). This is consistent with the previous demonstration that the  $\beta_2$ -AR interacts with the AKAP motifs of gravin- $\alpha$  (25). In contrast, HDAC11 was found to bind to the extreme carboxyl terminus of gravin- $\alpha$  (SI Appendix, Supplementary Index and Fig. S3 C and D) and, ultimately, to a 50-amino-acid region immediately adjacent to its two lysine targets in the PKA binding domain of gravin- $\alpha$  (Fig. 4 E and F). These findings suggest that gravin- $\alpha$  functions as a modular scaffold to regulate  $\beta$ -AR/PKA signaling in adipocytes in a manner that is regulated by HDAC11-reversible lysine acylation (Fig. 4G).

**Lysine Myristoylation of Gravin- $\alpha$  Is Required for  $\beta$ -AR-Mediated UCP1 Induction.** Specific AKAPs have not previously been linked to the regulation of  $\beta_3$ -AR signaling. Thus, gain- and loss-of-function experiments were performed with cultured cells to address the role of gravin- $\alpha$  and gravin- $\alpha$  myristoylation in the control of  $\beta_3$ -AR-mediated thermogenic gene expression in adipocytes (Fig. 5A). In 3T3-L1 adipocytes, lentiviral

overexpression of WT gravin- $\alpha$  increased UCP1 protein expression in the absence of exogenous signal and enhanced CL-mediated induction of the protein (Fig. 5B, lanes 1 through 8). In contrast, gravin- $\alpha$  KK/RR failed to stimulate UCP1 protein expression in unstimulated cells and blocked CL-mediated induction of UCP1, suggestive of dominant-negative action (Fig. 5B, lanes 9 through 16). Knockdown of endogenous gravin- $\alpha$  completely inhibited CL-induced expression of UCP1, and addback of WT, but not KK/RR gravin- $\alpha$ , rescued UCP1 expression (Fig. 5B, lanes 13 through 24). Immunoblotting with an anti-PKA substrates antibody revealed a remarkably similar pattern with WT, but not KK/RR, gravin- $\alpha$  enhancing and rescuing PKA signaling in 3T3-L1 adipocytes (Fig. 5C).

Studies were also performed with HIB1B cells to address whether the observed effects of gravin- $\alpha$  extend to brown adipocytes. As shown in Fig. 5D, ectopically expressed WT gravin- $\alpha$ , but not KK/RR, promoted UCP1 protein expression in the absence or presence of CL treatment (lanes 1 through 12). Knockdown of endogenous gravin- $\alpha$  expression blocked CL-mediated UCP1 induction, which was rescued by ectopic expression of WT but not KK/RR gravin- $\alpha$  (Fig. 5D, lanes 13

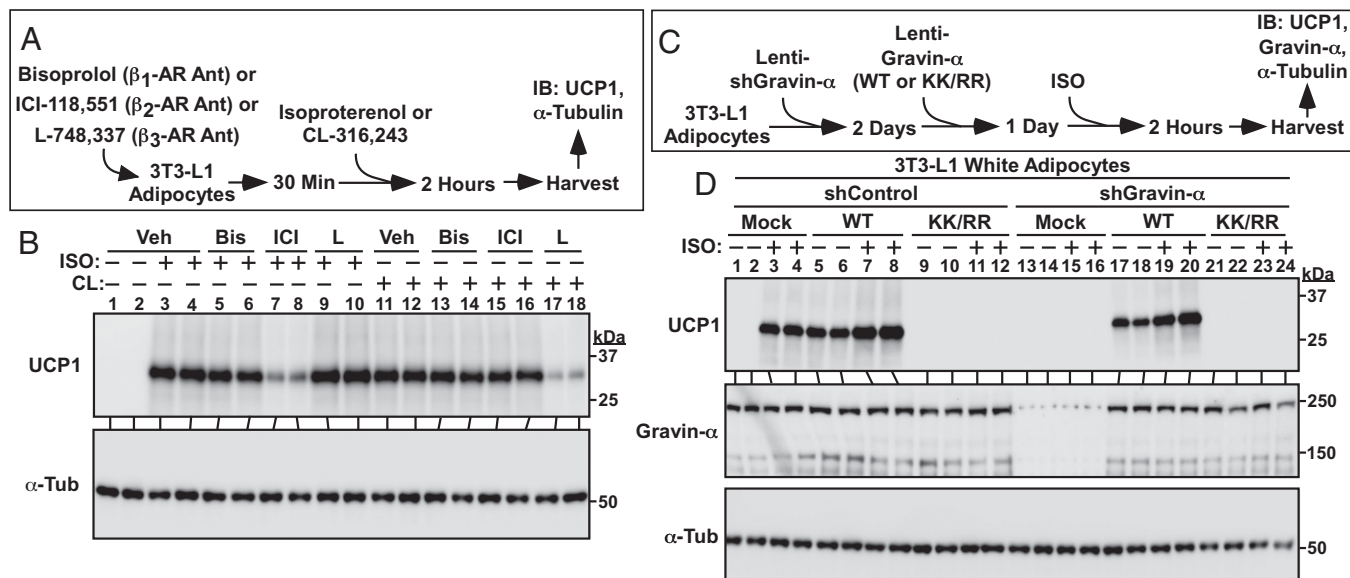


**Fig. 6.** Lysine myristoylation of gravin- $\alpha$  is required for  $\beta_2$ -AR-mediated UCP1 induction. (A) Schematic depiction of the experiment to address the roles of the three different  $\beta$ -AR isoforms in the control of UCP1 induction. Cells were pretreated with 10  $\mu$ M bisoprolol, 1  $\mu$ M ICI-118,551, or 10  $\mu$ M L-748,337, followed by addition of 1  $\mu$ M isoproterenol (ISO) or 1  $\mu$ M CL-316,243. (B) Immunoblot analysis of homogenates from 3T3-L1 adipocytes showing that ISO drives UCP1 induction via  $\beta_2$ -AR stimulation, while CL induces UCP1 by promoting  $\beta_3$ -AR signaling. Veh, vehicle; Bis, Bisoprolol; ICI, ICI-118,551; L, L-748,337. (C) Schematic depiction of the experiment to determine if gravin- $\alpha$  and its myristoylation are required for  $\beta_2$ -AR signaling in adipocytes. (D) Immunoblot analysis of UCP1 induction and gravin- $\alpha$  knockdown in 3T3-L1 adipocytes.  $\alpha$ -Tubulin ( $\alpha$ -Tub) served as a loading control. Please visit Figshare for a higher-resolution version (10.6084/m9.figshare.19082813).

through 24). Comparable to what was observed in 3T3-L1 white adipocytes, this pattern of UCP1 induction and repression in HIB1B brown adipocytes corresponded with PKA substrate phosphorylation (Fig. 5E).

A recent report highlighted the importance of adipocyte  $\beta_2$ -AR signaling for UCP1 induction in humans (32). As such, we addressed the possibility that gravin- $\alpha$  myristoylation also governs  $\beta_2$ -AR signaling in adipocytes. Treatment of 3T3-L1 cells with the  $\beta$ -AR agonist isoproterenol (ISO) in the absence or presence of  $\beta_1$ -,  $\beta_2$ -, or  $\beta_3$ -AR antagonists (Fig. 6A) established that under the employed experimental conditions, ISO drove UCP1 protein expression via  $\beta_2$ -AR stimulation (Fig. 6B, lanes 1 through 10); we also confirmed that CL-mediated UCP1 induction in 3T3-L1 adipocytes was via  $\beta_3$ -AR agonism (Fig. 6B, lanes 11 through 18). Next, gravin- $\alpha$  gain and loss of function were used to determine whether this AKAP controls  $\beta_2$ -AR responses in adipocytes (Fig. 6C). As was observed with CL, ISO-induced UCP1 protein expression was augmented by ectopically expressed WT gravin- $\alpha$  but was blocked by KK/RR (Fig. 6D, lanes 1 through 12). Likewise, knockdown of endogenous gravin- $\alpha$  completely suppressed ISO-mediated UCP1 induction, which was rescued by WT but not KK/RR gravin- $\alpha$  (Fig. 6D, lanes 13 through 24). Immunoblotting also revealed the requirement for gravin- $\alpha$  and its myristoylation in the regulation of ISO-induced PKA substrate phosphorylation (SI Appendix, Supplementary Index and Fig. S4). Together, these findings establish a requisite role for gravin- $\alpha$  myristoylation in the control of both  $\beta_2$ - and  $\beta_3$ -AR signaling in adipocytes.

**Lysine Myristoylation of Gravin- $\alpha$  Targets  $\beta_3$ -ARs to Caveolin-Rich Lipid Rafts.** We next sought to define the mechanism(s) by which lysine myristoylation of gravin- $\alpha$  promotes  $\beta$ -AR signaling in adipocytes. A cAMP-agarose pulldown assay revealed that gravin- $\alpha$  WT and KK/RR associated with endogenous PKA equivalently in either the absence or presence of HDAC11 inhibition (SI Appendix, Supplementary Index and Fig. S5), suggesting that diminished  $\beta$ -AR signaling in KK/RR-expressing cells was not due

to reduced binding of PKA to the scaffold. Prior studies demonstrated that adipocyte  $\beta_3$ -AR signaling is critically dependent on caveolin-1 (Cav-1), a scaffolding protein that is a component of cholesterol and sphingolipid-rich membrane lipid rafts (33–35). Thus, co-IP studies were performed to address whether gravin- $\alpha$  coordinates association of  $\beta_3$ -ARs with Cav-1 in adipocytes (Fig. 7A). Treatment of 3T3-L1 adipocytes with FT895 led to a profound increase in the association of FLAG-tagged WT gravin- $\alpha$  with endogenous Cav-1 and another lipid raft protein, Flotillin-2 (Flot-2) (Fig. 7B, lanes 5 through 10). In marked contrast, FT895 failed to stimulate association of gravin- $\alpha$  KK/RR with either lipid raft protein (Fig. 7B, lanes 11 through 16). Endogenous  $\beta_3$ -AR was equivalently associated with gravin- $\alpha$  WT and KK/RR in the absence or presence of FT895 treatment (Fig. 7B, Lower, lanes 5 through 16). Immunoblotting of cell homogenates confirmed that observed differences in the abundance of co-IPed proteins were not due to unequal inputs (Fig. 7C).

Stimulated emission depletion (STED) microscopy was performed to assess the subcellular distribution of gravin- $\alpha$  in 3T3-L1 adipocytes (Fig. 7D). Gravin- $\alpha$  WT and KK/RR were distributed throughout the cytoplasm, with enrichment at the plasma membrane. Concordant with the co-IP data, FT895 treatment led to redistribution of gravin- $\alpha$  WT to discrete regions of the cell periphery, where it colocalized with endogenous Cav-1 (Fig. 7E and F and SI Appendix, Supplementary Index and Fig. S64). In contrast, localization of gravin- $\alpha$  KK/RR was unaltered by the HDAC11 inhibitor.

The insolubility of cholesterol and sphingolipid-rich lipid rafts in nonionic detergents provides a biochemical means of identifying constituents of these membrane microdomains based on their detergent resistance and position within sucrose gradients (36, 37). To begin to address whether gravin- $\alpha$  lysine myristoylation impacts lipid raft targeting in adipocytes, 3T3-L1 cells were exposed to FT895 or vehicle control prior to homogenate preparation and sucrose gradient centrifugation. FT895 treatment led to significant enrichment of endogenous gravin- $\alpha$  and  $\beta_3$ -AR in detergent-resistant membranes (DRM), which

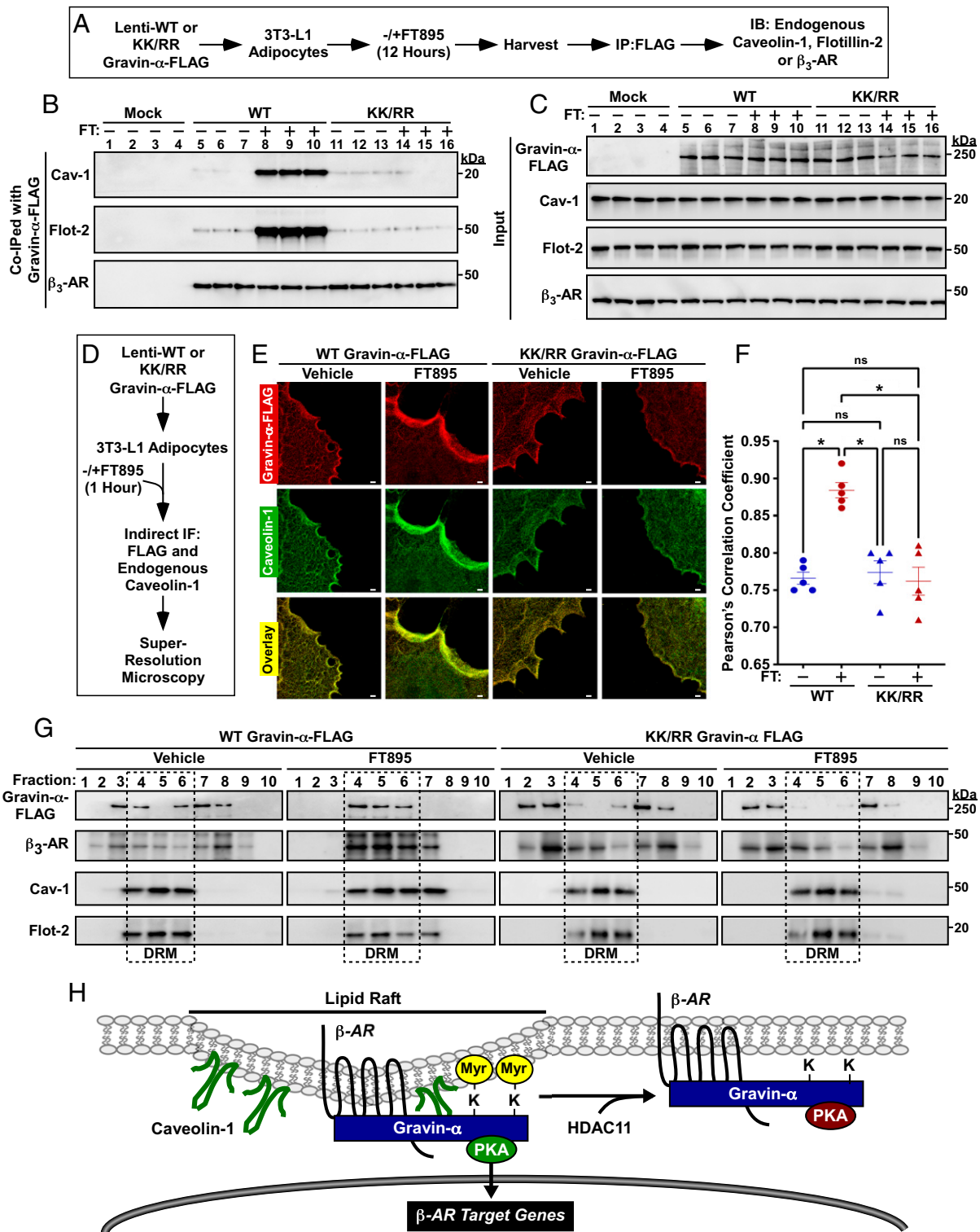


**Fig. 7.** Lysine myristoylation of gravin- $\alpha$  targets  $\beta_3$ -ARs to caveolin-rich lipid rafts. (A) Schematic depiction of the experiment to address whether lysine myristoylation of gravin- $\alpha$  regulates association with lipid raft proteins, Cav-1 and flotillin-2, and the  $\beta_3$ -AR. Cells were treated with 10  $\mu$ M FT895 or vehicle control. (B) Immunoblot analysis of proteins that coimmunoprecipitated with FLAG-tagged gravin- $\alpha$  WT or KK/RR in 3T3-L1 homogenates. FT, FT895. (C) Immunoblot analysis of input levels of the indicated proteins prior to immunoprecipitation. (D) Schematic depiction of the experiment to determine if HDAC11-reversible myristoylation alters the subcellular localization of gravin- $\alpha$  and/or Cav-1. (E) STED microscopy of FLAG-tagged gravin- $\alpha$  (red) and endogenous Cav-1 (green) in 3T3-L1 adipocytes treated with 10  $\mu$ M FT895 or vehicle control for 1 h. (Scale bar, 1,000 nm.) KK/RR, myristoylation-deficient. (F) Statistical analysis of the colocalization of ectopic gravin- $\alpha$  with endogenous Cav-1 using Pearson's correlation coefficient. Each dot represents one cell; center lines represent mean values. FT, FT895. \* $P < 0.05$ . ns = not significant. (G) Immunoblot analysis showing ectopic gravin- $\alpha$  and endogenous  $\beta_3$ -AR, Cav-1, and Flot-2 in fractions 1 through 10 from detergent-resistant membrane isolation in 3T3L1 adipocytes treated with 10  $\mu$ M FT895 or vehicle control for 12 h. (H) A model for the regulation of  $\beta$ -AR signaling in adipocytes by reversible lysine myristoylation. Myristoylation of gravin- $\alpha$  on two lysines in its PKA binding domain targets gravin- $\alpha$ : $\beta$ -AR:PKA complexes to Cav-1-rich lipid rafts, resulting in downstream signaling and induction of  $\beta$ -AR target genes, including that encoding UCP1. HDAC11-mediated demyristoylation of gravin- $\alpha$  prevents the complexes from localizing to the lipid rafts and thus squelches  $\beta$ -AR signaling. Please visit Figshare for a higher-resolution version (10.6084/m9.figshare.19082813).

also contained Flot-2 and Cav-1 (*SI Appendix, Supplementary Index and Fig. S6B*).

Follow-up studies were performed with 3T3-L1 adipocytes infected with lentiviruses expressing FLAG-tagged WT gravin- $\alpha$  or KK/RR. In vehicle-treated cells, gravin- $\alpha$  WT and KK/RR were widely distributed in multiple fractions from the sucrose gradient (Fig. 7G). In response to HDAC11 inhibition with FT895, FLAG-tagged WT gravin- $\alpha$  and endogenous  $\beta_3$ -AR collapsed into the three DRM fractions containing Flot-2 and Cav-1 (Fig. 7G, fractions 4 through 6). Similar to WT gravin- $\alpha$ , KK/RR was dispersed throughout the sucrose gradient in cells exposed to vehicle control. However, gravin- $\alpha$  KK/RR was strikingly resistant to FT895 treatment, remaining largely excluded from the DRM fractions, and this correlated with a lack of  $\beta_3$ -AR enrichment in these fractions (Fig. 7G). Taken together, these findings suggest that lysine myristoylation of gravin- $\alpha$  targets gravin- $\alpha$ : $\beta_3$ -AR:PKA complexes to lipid rafts in adipocytes.

## Discussion

Despite its recognition as a potent lysine demyristoylase, only one endogenous substrate of HDAC11 has previously been reported (14), and the biological functions of reversible lysine myristoylation in adipose tissue have not been described. Here, we define gravin- $\alpha$  as a second target of HDAC11 and demonstrate that this anchoring protein serves a crucial role in the control of adipocyte adrenergic signaling. Gravin- $\alpha$  loss of function in adipocytes blocks  $\beta$ -AR-mediated PKA signaling and downstream induction of the thermogenic gene product, UCP1.  $\beta$ -AR signaling can be rescued by reintroduction of WT gravin- $\alpha$  but not a myristoylation-deficient form of gravin- $\alpha$  harboring arginines in place of K1502 and K1505 (KK/RR). Collectively, our findings support a model in which HDAC11-reversible myristoylation of these two lysine residues targets gravin- $\alpha$ :PKA: $\beta$ -AR complexes to Cav-1-rich membrane lipid rafts, resulting in downstream signaling and expression of  $\beta$ -AR target genes (Fig. 7H).

HDAC11-mediated demyristoylation of gravin- $\alpha$  was observed in murine white and brown adipocytes, as well as in human subcutaneous adipocytes and VAT, suggesting a conserved role for lysine myristoylation/demyristoylation in the control of adipocyte signaling regardless of adipose depot. AKAPs are a family of >50 proteins that function as modular signaling platforms to mediate compartmentalized signaling and share a common ability to associate with PKA (38). The involvement of an AKAP in the control of adipocyte signaling was implied by the demonstration that Ht31, which is a broad-spectrum peptide inhibitor of PKA anchoring to AKAPs (39), blocked ISO-induced activation of PKA in 3T3-L1 cells, as determined using fluorescence resonance energy transfer reporter (40). However, the identity of the relevant AKAP and the mechanism(s) by which it regulates  $\beta$ -AR signaling in adipose tissue remained elusive.

Our findings reveal an obligatory role for gravin- $\alpha$  and lysine myristoylation of this AKAP in the control of  $\beta$ -AR signaling in adipocytes. Remarkably, K1502 and K1505 in gravin- $\alpha$  reside in a 13-amino-acid region that shows sequence identity with corresponding regions in other AKAPs and is predicted to form an amphipathic helix that contributes to binding to the PKA RII regulatory subunit (31). Conversion of K1502 and K1505 to arginines did not alter PKA binding to gravin- $\alpha$  but suppressed HDAC11 inhibitor-mediated translocation of gravin- $\alpha$  to distinct regions of the periphery of adipocytes, thereby blocking colocalization with the lipid raft component, Cav-1. Consistent with this, HDAC11 inhibition dramatically increased co-IP of WT but not KK/RR gravin- $\alpha$  with Cav-1 and another lipid raft component, Flot-2. Furthermore, HDAC11 inhibition triggered movement of gravin- $\alpha$ : $\beta$ -AR complexes containing WT but not KK/RR gravin- $\alpha$  to DRMs that are indicative of lipid rafts. We

hypothesize that the juxtaposition of PKA and membrane-embedded myristoyl-lysines of gravin- $\alpha$  positions the kinase in a microenvironment that facilitates its activation. The presence of an HDAC11 docking site immediately adjacent to the PKA binding domain in gravin- $\alpha$  provides a seemingly efficient means to demyristoylate the scaffold to squelch  $\beta$ -AR signaling.

Three isoforms of gravin/AKAP12 exist,  $\alpha$ ,  $\beta$ , and  $\gamma$ , which are encoded by independent transcripts under the control of separate promoters (29). HDAC11 likely regulates all gravin isoforms, since the three proteins have >95% amino acid sequence identity, with variability only shown to within their amino termini.

We previously demonstrated that HDAC11 suppresses UCP1 expression in adipocytes through association with BRD2 in the nucleus (17). This apparent redundancy may instead reflect unique, compartment-specific functions of the enzyme, with HDAC11-mediated demyristoylation of gravin- $\alpha$  blocking  $\beta$ -AR-mediated thermogenic gene expression and nuclear HDAC11 serving a more general role to repress basal UCP1 expression. Furthermore, given that  $\beta$ -AR-independent mechanisms for UCP1 induction exist, such as via the recently described GPCR3 (Gpr3) pathway (41), it is possible that nuclear HDAC11 functions as a nodal signaling integrator through which multiple pathways for thermogenic gene expression must pass in order to derepress UCP1 expression.

## Therapeutic Implications

Results of initial imaging studies confirming the presence of BAT that can be activated by cold temperature in humans further fueled interest in developing therapies for obesity based on increasing energy expenditure in BAT or “beige” WAT (42–46). Pharmacological approaches to promote BAT formation and function have focused heavily on the use of  $\beta_3$ -AR agonists (47). Nonetheless, while  $\beta_3$ -AR agonists were shown to acutely increase energy expenditure and insulin sensitivity in humans, they failed to promote weight loss upon chronic administration (21, 48–50). Results of more recent human studies with mirabegron, a  $\beta_3$ -AR agonist that is approved by the US Food and Drug Administration for the treatment of overactive bladder, have renewed interest in stimulating this GPCR pathway in adipose tissue as a means to treat metabolic disease (51–54). However, high doses of mirabegron were found to be required to promote BAT thermogenesis in humans, often resulting in increased blood pressure and heart rate, presumably due to off-target activation of  $\beta_1$ - and/or  $\beta_2$ -ARs (32).

Targeting of HDAC11 should be considered as an alternative or complementary strategy to augment thermogenesis in BAT and WAT to stimulate energy expenditure. HDAC11 is ostensibly a safe therapeutic target, since its global deletion in mice is well tolerated, and the discovery of FT895 (27), which is >10,000-fold selective for HDAC11 over other zinc-dependent HDACs, has established the feasibility of selectively inhibiting this enzyme. Because pharmacological inhibition of HDAC11 appears to stimulate thermogenic gene expression downstream of  $\beta$ -ARs, this approach could circumvent the toxic cardiovascular side effects associated with systemic  $\beta$ -AR agonist administration. In addition to inhibiting HDAC11 catalytic activity, an alternative strategy to promote thermogenesis could be to inhibit HDAC11 binding to gravin- $\alpha$ . In this regard, the HDAC11 docking site on gravin- $\alpha$  is  $\leq 50$  amino acids, suggesting the possibility of employing small-molecule ligands or peptides to disrupt the association to promote downstream signaling without affecting other HDAC11-mediated processes. Finally, the demonstration that ectopic expression of gravin- $\alpha$  is sufficient to stimulate UCP1 expression suggests the possibility of employing gravin- $\alpha$  gain-of-function gene therapy in adipose tissue as an approach to treat obesity.

Beyond adipose tissue and metabolic disease, pharmacological manipulation of gravin- $\alpha$  lysine myristoylation via HDAC11 inhibition may have other therapeutic applications. For example, in the heart, gravin- $\alpha$  regulates contractility (38) and  $\beta_3$ -AR agonists are cardioprotective, with mirabegron currently being tested for efficacy in patients with heart failure.  $\beta_3$ -AR signaling in cardiomyocytes was also recently shown to trigger activation of abhydrolase domain containing 5 (ABHD5), a lipid droplet-associated protease, resulting in cleavage of HDAC4 and suppression of an epigenetic program for pathological cardiac remodeling (55). Can HDAC11 inhibition recapitulate the salutary effects of  $\beta_3$ -AR agonists in the heart or provide added cardiac benefit as monotherapy or in combination with  $\beta_3$ -AR agonists? In the brain, gravin- $\alpha$  is protective in models of stroke (56, 57), and gravin- $\alpha$ -mediated PKA signaling promotes synaptic plasticity and memory storage (58), suggesting potential for HDAC11 inhibitors in neurological disorders. Enhancing gravin- $\alpha$  myristoylation could also lead to detrimental effects. For example,  $\beta_2$ -AR signaling has been linked to dysregulation of hepatic lipid metabolism and may contribute to the development of nonalcoholic fatty liver disease (59). The availability of FT895, which has pharmacokinetic properties that are suitable for in vivo studies (27), should facilitate efforts to determine the constellation of potential therapeutic indications for HDAC11 inhibitors and could uncover untoward consequences of inhibiting this lysine demyristoylase.

### Limitations of the Study

Our findings firmly establish a role for reversible lysine myristoylation of gravin- $\alpha$  in the control of  $\beta$ -AR signaling in adipocytes. However, since click chemistry with a tagged myristic acid was employed, we cannot rule out the involvement of other endogenous fatty acyl modifications that can be removed by HDAC11, such as palmitoyl, decanoyl, or dodecanoyl, in the regulation of gravin- $\alpha$ -mediated signaling (14–16). Furthermore, we did not address whether HDAC11 activity and/or localization are subject to signal-dependent control in response to  $\beta$ -AR agonists, nor whether  $\beta_1$ -AR signaling, which can stimulate UCP1 expression in human adipose tissue (60), is regulated by HDAC11. Finally, given that HDAC11 catalytic activity can be modulated by free

fatty acids and their coenzyme A derivatives in vitro (15), future studies should address whether this zinc-dependent HDAC functions as a metabolic sensor that couples nutrient availability to altered signal transduction and gene expression programs.

### Materials and Methods

Detailed descriptions of the materials and methods are provided in the *SI Appendix*. Briefly, 8-wk-old C57BL/6J male mice (JAX stock no. 000664) or 10- to 12-wk-old HDAC11-KO (or littermate WT) mice were used for in vivo studies following protocol approved by the Institutional Animal Care and Use Committee of the University of Colorado Anschutz Medical Campus. Human VAT and preadipocytes were procured under protocols approved by the Colorado Multiple Institutional Review Board. Lysine fatty acylation on gravin- $\alpha$  was detected using click chemistry. Lentiviruses were generated using commercially available plasmid constructs. Co-IP and immunoblotting were performed using total protein extracts. Stable isotope labeling using amino acids in cell culture labeling was performed using [ $^{13}\text{C}_6$ ,  $^{15}\text{N}_2$ ]-L-lysine and [ $^{13}\text{C}_6$ ,  $^{15}\text{N}_4$ ]-L-arginine. Statistical analyses were performed using GraphPad Prism 9.

**Data Availability.** All study data are included in the article and/or supporting information. Higher-resolution versions of the figures are available on Figshare (DOI: [10.6084/m9.figshare.19082813](https://doi.org/10.6084/m9.figshare.19082813)).

**ACKNOWLEDGMENTS.** We thank M. Felisbino for technical assistance and D. Klemm and C. Sucharov for advice. We thank T. Inge and B. Bergman for providing adipose tissue explants, R. Moldovan and D. Stich for assistance with microscopy, and J. Miano for rat gravin- $\alpha$  cDNA constructs. The confocal imaging experiments were performed in the Advanced Light Microscopy Core part of the NeuroTechnology Center at the University of Colorado Anschutz Medical Campus, supported in part by Rocky Mountain Neurological Disorders Core Grant No. P30 NS048154 and by Diabetes Research Center Grant No. P30 DK116073. The contents are the authors' sole responsibility and do not necessarily represent official NIH views. The STED microscope was funded through NSF Major Research Instrumentation Grant DBI-1337573 and NIH Shared Instrument Grant S10 RR023381. R.A.B. received funding from the Canadian Institutes of Health Research (Grant FRN-216927), and E.L.R. from the American Heart Association (Grant 829504). C.A.T. was supported by an NIH Training Grant (T32HL007822). B.K.M. received funding from the NIH (Grant HL141963) and the American Heart Association (Grant 18AIREA33960175) and a grant from the Robert J. Kleberg Jr. and Helen C. Kleberg Foundation. T.A.M. received funding from the NIH through grants HL116848, HL147558, DK119594, HL127240, and HL150225, and through a grant from the American Heart Association (165FRN31400013).

1. T. Kosciuk, H. Lin, *N*-myristoyltransferase as a glycine and lysine myristoyltransferase in cancer, immunity, and infections. *ACS Chem. Biol.* **15**, 1747–1758 (2020).
2. H. Jiang *et al.*, Protein lipidation: Occurrence, mechanisms, biological functions, and enabling technologies. *Chem. Rev.* **118**, 919–988 (2018).
3. M. D. Resh, Myristoylation and palmitoylation of Src family members: The fats of the matter. *Cell* **76**, 411–413 (1994).
4. C. Dian *et al.*, High-resolution snapshots of human *N*-myristoyltransferase in action illuminate a mechanism promoting N-terminal Lys and Gly myristoylation. *Nat. Commun.* **11**, 1132 (2020).
5. T. Kosciuk *et al.*, NMT1 and NMT2 are lysine myristoyltransferases regulating the ARF6 GTPase cycle. *Nat. Commun.* **11**, 1067 (2020).
6. F. T. Stevenson, S. L. Bursten, C. Fanton, R. M. Locksley, D. H. Lovett, The 31-kDa precursor of interleukin 1 alpha is myristoylated on specific lysines within the 16-kDa N-terminal propeptide. *Proc. Natl. Acad. Sci. U.S.A.* **90**, 7245–7249 (1993).
7. F. T. Stevenson, S. L. Bursten, R. M. Locksley, D. H. Lovett, Myristoylation of the tumor necrosis factor alpha precursor on specific lysine residues. *J. Exp. Med.* **176**, 1053–1062 (1992).
8. H. Jiang *et al.*, SIRT6 regulates TNF- $\alpha$  secretion through hydrolysis of long-chain fatty acyl lysine. *Nature* **496**, 110–113 (2013).
9. H. Jiang, X. Zhang, H. Lin, Lysine fatty acylation promotes lysosomal targeting of TNF- $\alpha$ . *Sci. Rep.* **6**, 24371 (2016).
10. X. Zhang, N. A. Spiegelman, O. D. Nelson, H. Jing, H. Lin, SIRT6 regulates Ras-related protein R-Ras2 by lysine defatty-acylation. *eLife* **6**, e25158 (2017).
11. S. A. Haws, C. M. Leech, J. M. Denu, Metabolism and the epigenome: A dynamic relationship. *Trends Biochem. Sci.* **45**, 731–747 (2020).
12. I. V. Gregoret, Y. M. Lee, H. V. Goodson, Molecular evolution of the histone deacetylase family: Functional implications of phylogenetic analysis. *J. Mol. Biol.* **338**, 17–31 (2004).
13. J. Du *et al.*, Sirt5 is a NAD-dependent protein lysine demethylase and desuccinylase. *Science* **334**, 806–809 (2011).
14. J. Cao *et al.*, HDAC11 regulates type I interferon signaling through defatty-acylation of SHMT2. *Proc. Natl. Acad. Sci. U.S.A.* **116**, 5487–5492 (2019).
15. Z. Kutil *et al.*, Histone deacetylase 11 is a fatty-acid deacylase. *ACS Chem. Biol.* **13**, 685–693 (2018).
16. C. Moreno-Yruela, I. Galleano, A. S. Madsen, C. A. Olsen, Histone deacetylase 11 is an  $\epsilon$ -N-myristoyllysine hydrolase. *Cell Chem. Biol.* **25**, 849–856.e8 (2018).
17. R. A. Bagchi *et al.*, HDAC11 suppresses the thermogenic program of adipose tissue via BRD2. *JCI Insight* **3**, e120159 (2018).
18. L. Sun *et al.*, Programming and regulation of metabolic homeostasis by HDAC11. *EBioMedicine* **33**, 157–168 (2018).
19. K. Y. Chen *et al.*, Opportunities and challenges in the therapeutic activation of human energy expenditure and thermogenesis to manage obesity. *J. Biol. Chem.* **295**, 1926–1942 (2020).
20. R. P. Ceddia, S. Collins, A compendium of G-protein-coupled receptors and cyclic nucleotide regulation of adipose tissue metabolism and energy expenditure. *Clin. Sci. (Lond.)* **134**, 473–512 (2020).
21. J. R. Arch, Challenges in  $\beta(3)$ -adrenoceptor agonist drug development. *Ther. Adv. Endocrinol. Metab.* **2**, 59–64 (2011).
22. S. R. Ross *et al.*, Hibernoma formation in transgenic mice and isolation of a brown adipocyte cell line expressing the uncoupling protein gene. *Proc. Natl. Acad. Sci. U.S.A.* **89**, 7561–7565 (1992).
23. F. Lin, Hy. Wang, C. C. Malbon, Gravin-mediated formation of signaling complexes in beta 2-adrenergic receptor desensitization and resensitization. *J. Biol. Chem.* **275**, 19025–19034 (2000).
24. M. Shih, F. Lin, J. D. Scott, H. Y. Wang, C. C. Malbon, Dynamic complexes of beta2-adrenergic receptors with protein kinases and phosphatases and the role of gravin. *J. Biol. Chem.* **274**, 1588–1595 (1999).
25. J. Tao, H. Y. Wang, C. C. Malbon, Protein kinase A regulates AKAP250 (gravin) scaffold binding to the beta2-adrenergic receptor. *EMBO J.* **22**, 6419–6429 (2003).
26. D. Willoughby, W. Wong, J. Schaack, J. D. Scott, D. M. Cooper, An anchored PKA and PDE4 complex regulates subplasmalemmal cAMP dynamics. *EMBO J.* **25**, 2051–2061 (2006).
27. M. W. Martin *et al.*, Discovery of novel N-hydroxy-2-arylisoindoline-4-carboxamides as potent and selective inhibitors of HDAC11. *Bioorg. Med. Chem. Lett.* **28**, 2143–2147 (2018).

28. X. Lin, E. Tomblar, P. J. Nelson, M. Ross, I. H. Gelman, A novel src- and ras-suppressed protein kinase C substrate associated with cytoskeletal architecture. *J. Biol. Chem.* **271**, 28430–28438 (1996).
29. J. W. Streb, C. M. Kitchen, I. H. Gelman, J. M. Miano, Multiple promoters direct expression of three AKAP12 isoforms with distinct subcellular and tissue distribution profiles. *J. Biol. Chem.* **279**, 56014–56023 (2004).
30. X. Yan, M. Walkiewicz, J. Carlson, L. Leiphon, B. Grove, Gravin dynamics regulates the subcellular distribution of PKA. *Exp. Cell Res.* **315**, 1247–1259 (2009).
31. J. B. Nauert, T. M. Klauk, L. K. Langeberg, J. D. Scott, Gravin, an autoantigen recognized by serum from myasthenia gravis patients, is a kinase scaffold protein. *Curr. Biol.* **7**, 52–62 (1997).
32. D. P. Blondin *et al.*, Human brown adipocyte thermogenesis is driven by  $\beta$ 2-AR stimulation. *Cell Metab.* **32**, 287–300.e7 (2020).
33. F. Ahmad *et al.*, Differential regulation of adipocyte PDE3B in distinct membrane compartments by insulin and the beta3-adrenergic receptor agonist CL316243: Effects of caveolin-1 knockdown on formation/maintenance of macromolecular signalling complexes. *Biochem. J.* **424**, 399–410 (2009).
34. A. W. Cohen *et al.*, Role of caveolin-1 in the modulation of lipolysis and lipid droplet formation. *Diabetes* **53**, 1261–1270 (2004).
35. M. Sato *et al.*, Interaction with caveolin-1 modulates G protein coupling of mouse  $\beta$ 3-adrenoceptor. *J. Biol. Chem.* **287**, 20674–20688 (2012).
36. D. A. Brown, Lipid rafts, detergent-resistant membranes, and raft targeting signals. *Physiology (Bethesda)* **21**, 430–439 (2006).
37. K. Simons, E. Ikonen, Functional rafts in cell membranes. *Nature* **387**, 569–572 (1997).
38. G. McConnachie, L. K. Langeberg, J. D. Scott, AKAP signaling complexes: Getting to the heart of the matter. *Trends Mol. Med.* **12**, 317–323 (2006).
39. D. W. Carr, Z. E. Hausken, I. D. Fraser, R. E. Stofko-Hahn, J. D. Scott, Association of the type II cAMP-dependent protein kinase with a human thyroid RII-anchoring protein. Cloning and characterization of the RII-binding domain. *J. Biol. Chem.* **267**, 13376–13382 (1992).
40. J. Zhang, C. J. Hupfeld, S. S. Taylor, J. M. Olefsky, R. Y. Tsien, Insulin disrupts beta-adrenergic signalling to protein kinase A in adipocytes. *Nature* **437**, 569–573 (2005).
41. O. Sveidahl Johansen *et al.*, Lipolysis drives expression of the constitutively active receptor GPR3 to induce adipose thermogenesis. *Cell* **184**, 3502–3518.e33 (2021).
42. M. K. Hankir, M. Klingenspor, Brown adipocyte glucose metabolism: A heated subject. *EMBO Rep.* **19**, e46404 (2018).
43. A. Pfeifer, L. S. Hoffmann, Brown, beige, and white: The new color code of fat and its pharmacological implications. *Annu. Rev. Pharmacol. Toxicol.* **55**, 207–227 (2015).
44. M. Saito *et al.*, High incidence of metabolically active brown adipose tissue in healthy adult humans: Effects of cold exposure and adiposity. *Diabetes* **58**, 1526–1531 (2009).
45. W. D. van Marken Lichtenbelt *et al.*, Cold-activated brown adipose tissue in healthy men. *N. Engl. J. Med.* **360**, 1500–1508 (2009).
46. K. A. Virtanen *et al.*, Functional brown adipose tissue in healthy adults. *N. Engl. J. Med.* **360**, 1518–1525 (2009).
47. G. Schena, M. J. Caplan, Everything you always wanted to know about  $\beta$ 3-AR \* (\* But were afraid to ask). *Cells* **8**, E357 (2019).
48. T. M. Larsen *et al.*, Effect of a 28-d treatment with L-796568, a novel beta(3)-adrenergic receptor agonist, on energy expenditure and body composition in obese men. *Am. J. Clin. Nutr.* **76**, 780–788 (2002).
49. M. A. van Baak *et al.*, Acute effect of L-796568, a novel beta 3-adrenergic receptor agonist, on energy expenditure in obese men. *Clin. Pharmacol. Ther.* **71**, 272–279 (2002).
50. C. Weyer, P. A. Tataranni, S. Snitker, E. Danforth Jr., E. Ravussin, Increase in insulin action and fat oxidation after treatment with CL 316,243, a highly selective beta3-adrenoceptor agonist in humans. *Diabetes* **47**, 1555–1561 (1998).
51. A. S. Baskin *et al.*, Regulation of human adipose tissue activation, gallbladder size, and bile acid metabolism by a  $\beta$ 3-adrenergic receptor agonist. *Diabetes* **67**, 2113–2125 (2018).
52. A. M. Cypess *et al.*, Activation of human brown adipose tissue by a  $\beta$ 3-adrenergic receptor agonist. *Cell Metab.* **21**, 33–38 (2015).
53. J. S. Flier, Might  $\beta$ 3-adrenergic receptor agonists be useful in disorders of glucose homeostasis? *J. Clin. Invest.* **130**, 2180–2182 (2020).
54. A. E. O'Mara *et al.*, Chronic mirabegron treatment increases human brown fat, HDL cholesterol, and insulin sensitivity. *J. Clin. Invest.* **130**, 2209–2219 (2020).
55. Z. H. Jebessa *et al.*, The lipid droplet-associated protein ABHD5 protects the heart through proteolysis of HDAC4. *Nat. Metab.* **1**, 1157–1167 (2019).
56. J. H. Cha *et al.*, AKAP12 mediates barrier functions of fibrotic scars during CNS repair. *PLoS One* **9**, e94695 (2014).
57. J. H. Cha *et al.*, Prompt meningeal reconstruction mediated by oxygen-sensitive AKAP12 scaffolding protein after central nervous system injury. *Nat. Commun.* **5**, 4952 (2014).
58. R. Havekes *et al.*, Gravin orchestrates protein kinase A and  $\beta$ 2-adrenergic receptor signaling critical for synaptic plasticity and memory. *J. Neurosci.* **32**, 18137–18149 (2012).
59. Y. Shi *et al.*,  $\beta$ 2-adrenergic receptor agonist induced hepatic steatosis in mice: Modeling nonalcoholic fatty liver disease in hyperadrenergic states. *Am. J. Physiol. Endocrinol. Metab.* **321**, E90–E104 (2021).
60. M. J. Riis-Vestergaard *et al.*, Beta-1 and not beta-3 adrenergic receptors may be the primary regulator of human brown adipocyte metabolism. *J. Clin. Endocrinol. Metab.* **105**, dgz298 (2020).